

CENTRAL COMPOSITE FACE-CENTERED DESIGN-BASED OPTIMISATION, DEVELOPMENT AND CHARACTERISATION OF FAVIPIRAVIR-LOADED PLGA NANOPARTICLES

VENKATA KAVYA R.*, JEEVANA JYOTHI B.

Department of Pharmaceutics, Institute of Pharmaceutical Technology, Sri Padmavati Mahila Visvavidyalayam (Women's University),
Tirupati, Andhra Pradesh, India
*Email: kavyarenisetty1996@gmail.com

Received: 06 Sep 2022, Revised and Accepted: 18 Oct 2022

ABSTRACT

Objective: The objective of this study is to fabricate favipiravir-loaded PLGA nanoparticulate systems that can increase the solubility along with the sustained release of favipiravir.

Methods: The favipiravir-loaded Poly (D, L-lactic-co-glycolide) (PLGA) nanoparticulate systems were prepared by the nanoprecipitation method. A 3-factor, 2-level central composite face-centered design was employed to study the effect of formulation variables having a concentration of PLGA, polyvinyl alcohol (PVA) and stirring rate as critical formulation attributes and particle size, drug entrapment efficiency, and percentage cumulative drug release as critical quality attributes on prepared favipiravir nanoparticles. Drug interaction studies were performed by FTIR and DSC. Surface morphology was analysed by scanning electron microscopy (FEI Quanta 250 FEG, USA). Particle size, zeta potential, and polydispersity index were analysed by the nanoparticle analyser SZ-100 (HORIBA Scientific nanopartica, Japan). *In vitro* drug release studies were performed using a UV-Visible spectrophotometer at λ_{max} 234 nm. *In vitro* drug release data obtained was fitted into various mathematical kinetic models.

Results: The numerical optimization process predicted the level of PLGA concentration as 69.96 mg, PVA concentration as 4.99%, and stirring rate as 799 rpm for the optimised formulation. The low percentage of relative error for the optimised formulation confirms the validation of the model. The optimised formulation had a 77.65% entrapment efficiency with a particle size of 109.7 nm and the percent cumulative drug release showed 86.46% drug release over 720 min. The drug release was found to follow first-order release kinetics with anomalous non-Fickian diffusion kinetics.

Conclusion: Hence, such an attempt at fabrication of favipiravir-loaded PLGA nanoparticulate systems may be useful for sustained release of drug over 720 min.

Keywords: Favipiravir, PLGA, Central composite design

© 2023 The Authors. Published by Innovare Academic Sciences Pvt Ltd. This is an open-access article under the CC BY license (<https://creativecommons.org/licenses/by/4.0/>)
DOI: <https://dx.doi.org/10.22159/ijap.2023v15i1.46289>. Journal homepage: <https://innovareacademics.in/journals/index.php/ijap>

INTRODUCTION

Favipiravir is a prodrug (T-705) with a low molecular weight and a potent inhibitor of RNA-dependent RNA polymerase (RdRp) of RNA viruses. In different types of RNA viruses, RNA-dependent RNA polymerase exists, which enables a broader spectrum of antiviral activities of favipiravir [1]. The limitation with favipiravir is that it belongs to a BCS class IV drug and has a short half-life of 2–5.5 h following oral administration [2]. The poor solubility and short half-life of favipiravir lead to an increased requirement of daily high doses of 1600 mg twice daily to get the therapeutic benefits from orally administered favipiravir formulations. By incorporating it into nanoparticulate systems, it might enable favipiravir to be present in the biological system for a longer period of time due to its sustained drug delivery [3].

Nanotechnology is being quickly adopted by the pharmaceutical industry. One of the main applications of nanotechnology is the nano-encapsulation of pharmaceutically active compounds. The nano-encapsulation technique boosts the particle's surface-to-volume ratio, which in turn boosts the bioavailability of compounds, in addition to offering protection [4, 5]. Nanoparticles are submicron-sized particles with therapeutic agents dispersed, adsorbed, or encapsulated in polymeric matrices or vesicles. The small particle size and high specific surface area of nanoparticles enable greater drug loading and access into host cells, boosting the efficacy of antiviral medications. This facilitates the development of sophisticated drug delivery systems. Polymeric nanoparticles such as PLGA nanoparticles exhibit ideal characteristics for an effective drug delivery vehicle and are versatile due to their biocompatibility in encapsulating different drugs. Polysaccharides (like chitosan, sodium alginate, and starch), and synthetic polymers (like poly (d, l-lactide), poly (lactic acid), poly (d, l-glycolide), poly (lactide-co-glycolide), and poly (cyanoacrylate)

PCA) can all be used to make biodegradable polymeric nanoparticles [6, 7].

Previously, favipiravir was formulated as an aerosolized nano-formulation [8], favipiravir nanoclusters [9], proliposomal powder for pulmonary delivery [10], and mouth-dissolving tablets [11]. According to the literature review, PLGA nanoparticles of favipiravir have not yet been developed. These favipiravir-loaded PLGA nanoparticles prolong the systemic circulation time and control the drug delivery. Hence, in the present study, an attempt was made to develop nanoparticulate systems of the poorly water-soluble drug favipiravir using PLGA as a polymer, which is expected to improve the solubility and dissolution properties of the drug [12].

MATERIALS AND METHODS

Favipiravir is obtained as a gift sample from INCHEM Laboratories Pvt. Ltd., Hyderabad, India. Poly (D, L-lactic-co-glycolide)-PLGA 50:50 was purchased from Nomisma Healthcare Pvt. Ltd., Vadodra, India. Polyvinyl alcohol-PVA was obtained from SD Fine Chem, Mumbai, India. All other reagents and solvents used were of analytical grade.

Fabrication of favipiravir-loaded PLGA nanoparticles

Favipiravir-loaded PLGA nanoparticles were prepared by the nanoprecipitation method. Polymer-to-drug ratios range from 1:2, 1:4, and 3:4. Favipiravir and PLGA were dissolved in 5 ml of acetone, which was then added drop-wise using a syringe at a flow rate of 1 ml/min to 25 ml of an aqueous solution containing PVA. It was kept under continuous stirring for 4 h using a homogeniser to allow complete evaporation of acetone, leaving a colloidal suspension of favipiravir-loaded PLGA nanoparticles. To remove untrapped drug, the colloidal suspension was centrifuged at 10,000 rpm for 30 min and washed twice with distilled water. Then it was filtered and

lyophilized for 2 d using a lyophilizer. The lyophilized favipiravir-loaded PLGA nanoparticles were kept in a desiccator for further evaluation studies [13-15].

Experimental design

A 3 factor, 2 level, the face-centered central composite design was employed to optimise formulation and process parameters for the preparation of favipiravir-loaded PLGA nanoparticles. All three variables were taken at two levels, high and low, which were represented by coded values of +1 and -1, respectively. Six runs of

replicates were performed at the centre point coded 0 to estimate the overall curvature effect and experimental error. Design-Expert software (Version 13.0.12.0 Trail, Stat Ease Inc, USA) was employed for the generation and evaluation of the 20 experimental runs given in table 1. For optimization of favipiravir nanoparticles, critical formulation attributes were identified to be the polymer (PLGA) fraction, the concentration of stabiliser (PVA), stirring rate, and desired critical quality attributes like particle size (R1), drug entrapment efficiency (R2), and cumulative percentage drug release at 720 min (R3) were selected [16, 17].

Table 1: Composition of experimental runs of favipiravir-loaded PLGA nanoparticles

Experimental run	Favipiravir (mg)	Concentration of PLGA (mg)	Concentration of PVA (%)	Stirring rate (rpm)
FNP01	200	150	5	400
FNP02	200	50	5	400
FNP03	200	150	3	600
FNP04	200	100	5	600
FNP05	200	100	3	400
FNP06	200	50	1	400
FNP07	200	100	3	600
FNP08	200	100	3	800
FNP09	200	100	1	600
FNP010	200	100	3	600
FNP011	200	100	3	600
FNP012	200	100	3	600
FNP013	200	50	3	600
FNP014	200	100	3	600
FNP015	200	150	1	800
FNP016	200	100	3	600
FNP017	200	50	1	800
FNP018	200	150	1	400
FNP019	200	150	5	800
FNP020	200	50	5	800

Statistical analysis of critical quality attributes by design expert

Multiple regression analysis was employed to study the effects of factors and their interactions on observed responses by means of polynomial models. Equation 1 represents a second-order polynomial equation, where R is the calculated response connected with each critical formulation attribute level combination. b_0 is the arithmetic mean response of all experimental runs. The polynomial terms b_1, b_2, b_3 are coefficients of main effects A (PLGA concentration), B (PVA concentration), and C (stirring rate) to understand the average result of changing one factor at a time from its low value to its high value. The polynomial terms b_{12}, b_{13}, b_{23} are coefficients of interaction terms AB, AC, BC, which describe the change in response when two factors are altered simultaneously. To study the nonlinearity of the model, $b_{11}, b_{22},$ and b_{33} are required. Each coefficient carries a mathematical sign. A positive sign indicates a synergistic effect and a negative sign represents an antagonistic effect.

$$R = b_0 + b_1A + b_2B + b_3C + b_{12}AB + b_{13}AC + b_{23}BC + b_{11}A^2 + b_{22}B^2 + b_{33}C^2 \dots$$

Equation.1

Based on comparisons of statistical parameters, the best fit model was selected. For each response, ANOVA was calculated to determine the significance of each parameter selected for the study by using probability value (p-value). Perturbation plots, 3D Response surface plots, and 2D contour plots were analysed to visualise the effects of critical formulation attributes and their interactions on responses [18, 19].

Numerical and graphical optimization

A desirability approach was used to develop an optimised formulation with desired responses by employing numerical and graphical optimisation techniques. For calculating desirability "D", the desired goal like minimum, maximum, target, or the in-range value was chosen for each response, and the goals were combined into a simultaneous objective function to yield a desirability plot. An optimised formulation with optimised conditions was derived with the help of a desirability plot and ramp solutions. Optimised

formulation experimental values for responses were correlated with the predicted values generated by the Design-Expert software (Version 13.0.12.0 Trail, Stat Ease Inc, USA) to determine the percentage of predicted error. The percentage predicted error should be less than $\pm 2\%$ to be within the acceptable limits [20, 21].

Characterization of favipiravir loaded plga nanoparticles

Fourier transform infrared spectroscopy, differential scanning calorimetry, surface morphological analysis, particle size, zeta potential, drug entrapment efficiency, and *in vitro* drug release testing were used to characterise all of the prepared favipiravir formulations.

Fourier transform infrared spectroscopy

To investigate the stability of favipiravir within polymeric materials, the FTIR spectra of pure drug favipiravir and a promising formulation were recorded using an IR spectrophotometer and the pressed pellet technique. Samples were prepared by pressing them with KBr into pellets. In this study, the spectra obtained for pure favipiravir and a promising formulation were scanned between wave number regions of 4000-400 cm^{-1} [22].

Differential scanning calorimetry

The thermal behaviour of pure favipiravir and the optimised formulation were analysed using a differential scanning calorimeter. 10 mg of sample was placed in aluminium crimp cells and subjected to DSC under constant purging of nitrogen at 20 ml/min. Thermograms were recorded by heating samples from 100 to 250 $^{\circ}\text{C}$ at a heating rate of 10 $^{\circ}\text{C}/\text{min}$ with an empty aluminium pan as the reference [23].

Surface morphology

The morphological characteristics of the favipiravir-loaded PLGA nanoparticles were determined by performing analysis using scanning electron microscopy (FEI Quanta 250 FEG, USA). For SEM analysis, favipiravir-loaded PLGA nanoparticles were positioned

onto a brass stub and sputtered with gold using gold coating-Quorum, later fixed into a sample holder, then examined under low vacuum (1023 mm HG) and photographed randomly [24].

Particle size, polydispersity index and zeta potential

Particle size, zeta potential, and polydispersity index were estimated by a nanoparticle analyser for prepared nanoparticle formulations. The prepared favipiravir-loaded PLGA nanoparticles were diluted with ultra-pure water to yield a suitable scattering intensity. Diluted nanoparticle dispersion was poured into a cuvette, which was placed in the cuvette holder of the instrument and analysed using zeta sizer software. Folded capillary cuvette was used for zeta potential measurement [25].

Determination of drug entrapment efficiency

10 mg of lyophilized favipiravir-loaded PLGA nanoparticles were accurately weighed and placed in 10 ml of 50 mmol phosphate buffer of pH 6.8. The solution was sonicated for 30 min and the final volume was made up to 25 ml with 50 mmol phosphate buffer of pH 6.8 and kept for 24 h. The supernatant was estimated for drug content using a UV-Visible spectrophotometer (Shimadzu UV 1800, Japan) at λ_{\max} 234 nm. Drug entrapment efficiency was expressed as the percentage of drug in the fabricated favipiravir-loaded PLGA nanoparticles with respect to the initial amount of favipiravir used for the preparation of nanoparticles given in equation 2 [26].

$$\text{Drug Entrapment Efficiency} = \frac{\text{Total amount of drug initially added} - \text{drug in supernatant (mg)}}{\text{Total amount of drug initially added (mg)}} \times 100 \text{ Equation 2}$$

In vitro drug release testing

In vitro drug release studies of favipiravir from favipiravir-loaded nanoparticles were performed for all the prepared nanoparticles. Powders equivalent to containing 200 mg of favipiravir were taken in a cellulose dialysis membrane (molecular weight cut-off of 12000 Da, Himedia, Mumbai, India), which was hermetically sealed and tied to a USP type II paddle of dissolution testing apparatus (Electrolab, India) before being immersed into 900 ml of 50 mmol phosphate buffer of pH 6.8, which acts as the dissolution medium. The

temperature was maintained at $37 \pm 0.5 \text{ }^\circ\text{C}$ with 100 rpm. Samples of 5 ml were withdrawn at predetermined time intervals and replaced by the same volume of phosphate buffer of pH 6.8 to maintain sink conditions. The concentration of favipiravir released was determined spectrophotometrically at λ_{\max} of 234 nm. All the experiments were performed in triplicate, and the average values were recorded [27, 28].

Kinetic release mechanism

To understand the mechanism and kinetics of drug release, the *in vitro* drug release data obtained was fitted into various mathematical kinetic models such as zero order, first order, and the Higuchi and Korsmeyer peppas model. On the X-axis and Y-axis, the zero-order (cumulative percentage of drug released Vs time), first-order (log cumulative percentage of drug retained Vs time), Higuchi (cumulative percentage of drug released Vs square root of time), and Korsmeyer peppas models (log cumulative percentage of drug released Vs log time) were considered [29].

RESULTS AND DISCUSSION

Fabrication of favipiravir-loaded PLGA nanoparticles

By employing the nanoprecipitation method, favipiravir-loaded PLGA nanoparticles were fabricated successfully for sustained release. This method employs biodegradable polymer, which can be easily eliminated from the body. It was a simple technique when compared with other solvent-based preparation methods and resulted in better entrapment efficiency.

Experimental design

The central composite design is the most popular response surface model used to design and optimise the experiments while analysing the interaction effects and quadratic effects. In the present study, three factors at two levels of face-centered central composite design were employed with experimental runs performed at 20 combinations, each of which contains 6 replicates to estimate the experimental error and curvature effect [30]. The results of responses obtained for 20 experimental runs designed based on the central composite design are depicted in table 2.

Table 2: Central composite design layout with responses for favipiravir-loaded PLGA nanoparticles

Experimental Runs	Favipiravir (mg)	Factor 1 A: PLGA concentration (mg)	Factor 2 B: PVA concentration (%)	Factor 3 C: stirring rate (rpm)	Response 1 particle size (nm)	Response 2 Drug entrapment efficiency (%)	Response 3 cumulative percentage drug release at 720 min (%)
FNP01	200	150	5	400	268.8	96.82	62.84
FNP02	200	50	5	400	108.4	72.36	96.48
FNP03	200	150	3	600	248.7	98.42	68.89
FNP04	200	100	5	600	156.6	87.26	71.65
FNP05	200	100	3	400	149.6	81.98	87.65
FNP06	200	50	1	400	123.6	64.6	94.58
FNP07	200	100	3	600	189.9	86.35	78.25
FNP08	200	100	3	800	149.2	82.6	85.49
FNP09	200	100	1	600	209.3	80.16	74.25
FNP010	200	100	3	600	182.6	84.52	78.25
FNP011	200	100	3	600	188.5	86.39	78.39
FNP012	200	100	3	600	182.0	86.46	81.89
FNP013	200	50	3	600	119.7	74.75	92.58
FNP014	200	100	3	600	182.6	84.35	82.61
FNP015	200	150	1	800	226.9	92.34	73.56
FNP016	200	100	3	600	202.8	85.98	80.62
FNP017	200	50	1	800	119.5	69.91	97.62
FNP018	200	150	1	400	286.4	88.92	62.98
FNP019	200	150	5	800	199.5	95.82	65.68
FNP020	200	50	5	800	98.7	75.36	91.47

Statistical analysis of critical quality attributes by design expert

For statistical analysis, all the observed values for critical quality attributes (particle size, drug entrapment efficiency, and cumulative percentage drug release at 720 min) of 20 experimental runs were fitted to various models such as linear, 2FI (two-factor interaction),

quadratic, and cubic for statistical analysis. ANOVA revealed a statistically significant relationship between the factors and the responses. A significant polynomial model was selected by considering statistical parameters such as correlation coefficient (R^2), adjusted R^2 , predicted R^2 , and predicted residual sum of squares (PRESS), and the results are presented in table 3 [31].

Table 3: Selection of appropriate model by using design expert

R1-particle size						
Model type	p-value	R ²	Adjusted R ²	Predicted R ²	PRESS	Remarks
Linear	<0.0001	0.9002	0.8815	0.8307	8925.92	
2FI	0.1556	0.9324	0.9011	0.8674	6990.87	
Quadratic	0.0845	0.9641	0.9319	0.8040	10332.30	Suggested
Cubic	0.3278	0.9817	0.9421	-14.0895	7.955E+05	Aliased
R2-Drug entrapment efficiency						
Model type	p-value	R ²	Adjusted R ²	Predicted R ²	PRESS	Remarks
Linear	<0.0001	0.9445	0.9341	0.9049	145.40	
2FI	0.6220	0.9514	0.9289	0.7388	399.19	
Quadratic	<0.0001	0.9949	0.9904	0.9752	37.90	Suggested
Cubic	0.5312	0.9968	0.9899	0.7690	353.01	Aliased
R3-Cumulative percentage drug release at 720 min						
Model type	p-value	R ²	Adjusted R ²	Predicted R ²	PRESS	Remarks
Linear	<0.0001	0.8705	0.8462	0.7936	463.99	
2FI	0.3534	0.8983	0.8514	0.8344	372.16	
Quadratic	0.0004	0.9822	0.9661	0.9178	184.84	Suggested
Cubic	0.2946	0.9913	0.9725	0.9508	110.67	Aliased

All the responses for favipiravir-loaded PLGA nanoparticles followed the quadratic model. Fit statistics for the selected models for all the critical quality attributes (particle size R1, drug entrapment efficiency R2, cumulative percentage drug release at 720 min R3) are given in table 4. The coefficient of variance values for all the responses R1, R2, and R3 were found to be less than 10%, which indicates the reproducibility of the respective models. Adequate

precision for all the responses R1, R2, and R3 was found to be greater than 4, which indicates an adequate signal and all the models can be used to navigate the design space. The lack of fit F values of 4.96, 0.6792, and 1.06 for R1, R2, and R3, respectively, implies the lack of fit F values are not significant relative to the pure error which could occur due to noise. Because a non-significant lack of fit is good, the respective models were fit [32].

Table 4: Fit statistics for selected models for all critical quality attributes

Responses	Model	Standard deviation	Mean	C. V. %	Adequate precision	Lack of fit F-value
R1	Quadratic	13.75	179.67	7.65	19.2801	4.96
R2	Quadratic	0.8797	83.77	1.05	54.6069	0.6792
R3	Quadratic	2.00	80.29	2.49	23.0427	1.06

Statistical parameters and coefficients of model terms obtained for the quadratic model for the studied responses R1, R2, and R3 are shown in table 5. The mathematical models generated the Design

Expert software after removing insignificant terms ($p > 0.05$) for the responses are represented as reduced quadratic models and were discussed in the explanation of the respective responses [33].

Table 5: Summary of ANOVA for all critical quality attributes

Source	Sum of squares	Degree of freedom	Mean square	F value	P value
R1-particle size					
Model	50827.21	9	5647.47	29.88	<0.0001(S)
A	43626.03	1	43626.03	230.79	<0.0001(S)
B	1787.57	1	1787.57	9.46	0.0117 (S)
-C	2044.90	1	2044.90	10.82	0.0082 (S)
AB	10.12	1	10.12	0.0536	0.8216 (NS)
AC	1653.12	1	1653.12	8.75	0.0144 (S)
BC	29.64	1	29.64	0.1568	0.7004 (NS)
A ²	285.35	1	285.35	1.51	0.2473 (NS)
B ²	217.16	1	217.16	1.15	0.3090 (NS)
C ²	1672.81	1	1672.81	8.85	0.0139 (S)
R2-Drug entrapment efficiency					
Model	1520.66	9	168.96	218.35	<0.0001 (S)
A	1330.33	1	1330.33	1719.20	<0.0001 (S)
B	100.43	1	100.43	129.78	<0.0001 (S)
C	12.88	1	12.88	16.65	0.0022 (S)
AB	0.4186	1	0.4186	0.5410	0.4789 (NS)
AC	4.34	1	4.34	5.60	0.0395 (S)
BC	5.66	1	5.66	7.32	0.0221 (S)
A ²	3.90	1	3.90	5.04	0.0486 (S)
B ²	7.80	1	7.80	10.08	0.0099 (S)
C ²	26.50	1	26.50	34.24	0.0002 (S)
R3-Cumulative percentage drug release at 720 min					
Model	2207.78	9	245.31	61.21	<0.0001 (S)
A	1925.99	1	1925.99	480.56	<0.0001 (S)
B	22.11	1	22.11	5.52	0.0407 (S)
C	8.63	1	8.63	2.15	0.1730 (NS)
AB	1.78	1	1.78	0.4433	0.5206 (NS)
AC	29.61	1	29.61	7.39	0.0216 (S)
BC	31.17	1	31.17	7.78	0.0192 (S)
A ²	2.12	1	2.12	0.5297	0.4834 (NS)
B ²	131.17	1	131.17	32.73	0.0002 (S)
C ²	123.95	1	123.95	30.93	0.0002 (S)

Effect of factors on particle size (R1)

The correlation between the chosen critical formulation attributes and critical quality attributes was established as per the generated polynomial equation for response R1-particle size, shown in equation 3

$$R1 = 182.47 + 66.05A - 13.37B - 14.30C - 14.38AC - 24.66C^2 \text{ Eq. 3}$$

As per the coefficients of model term values from equation. 3 and their signs, it is evident that the individual impact of concentration of PLGA (A) has a significant positive effect and that concentration of PVA (B), stirring rate (C), interaction term (AC), and square coefficient of stirring rate (C^2) have a significant negative effect on particle size. Hence, the particle size will increase with an increase in the concentration of PLGA and decrease with a synergistic rise in the concentration of PVA and stirring rate. It was found that the effect of PLGA concentration was greater than the change in concentration of PVA and stirring rate on particle size. The effect of the three variables on the particle size can be arranged in the sequence $A > C > B$. Thus, optimum values of A, B, and C are important for obtaining a desirable particle size for favipiravir-loaded PLGA nanoparticles [34].

An increase in the PLGA concentration led to an increase in the organic phase viscosity, which hinders the dispersion of the organic

phase into the aqueous phase, thereby promoting the formation of larger droplets. Sahin A. *et al.*, proposed a similar inference where an increase in the polymer fraction increases the particle size due to slow diffusion of solvent into the external phase with an increase in organic phase viscosity [35]. The nanoparticle size dramatically decreased with an increase in PVA concentration due to enhanced interfacial stabilisation as PVA molecules stabilise and prevent the aggregation of nanoparticles. Particle size increases with decreased PVA concentration due to reduced interfacial stability resulting from an insufficient amount of stabilizer, leading to the aggregation of particles, and similar results were demonstrated by R. M. Mainardes *et al.* [36]. An increase in stirring rate significantly decreases the particle size of favipiravir-loaded PLGA nanoparticles due to faster removal of organic solvent that decreases the aggregation of nanoparticles, thus promoting the smaller size particles [37].

To visualise the relationship between particle size and formulation attributes (A-PLGA concentration, B-PVA concentration, C-stirring rate), model graphs, namely perturbation charts, three-dimensional surface plots, and contour plots, were generated. From the perturbation chart fig. 1a, it is evident that increasing the concentration of PLGA will increase the particle size of PLGA nanoparticles. The semi-planar three-dimensional surface plot fig. 1b and the curve in the contour plot fig. 1c also assure the same [38].

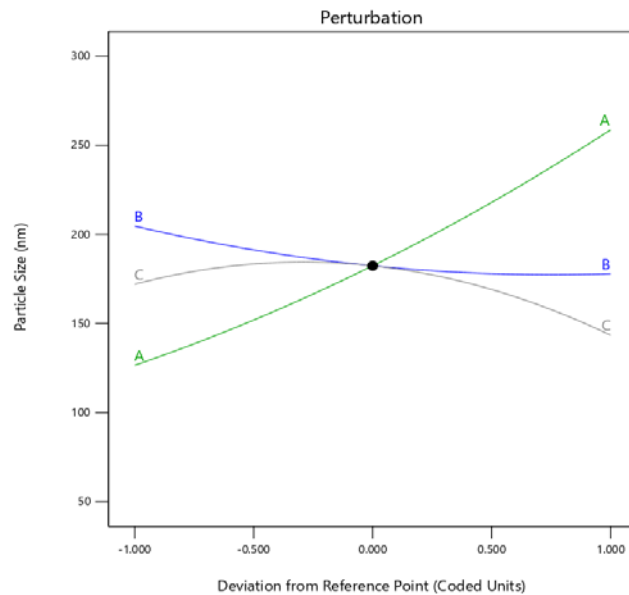


Fig. 1a: Perturbation chart of particle size

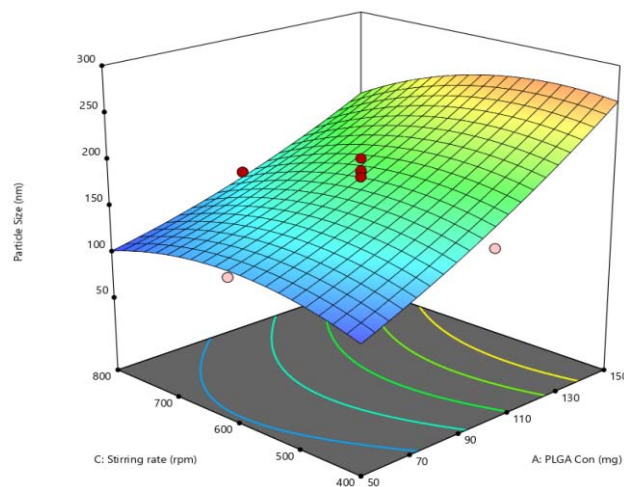


Fig. 1b: Three-dimensional surface plot for particle size as a function of the formulation variables: (A) concentration of PLGA and (C) Stirring rate

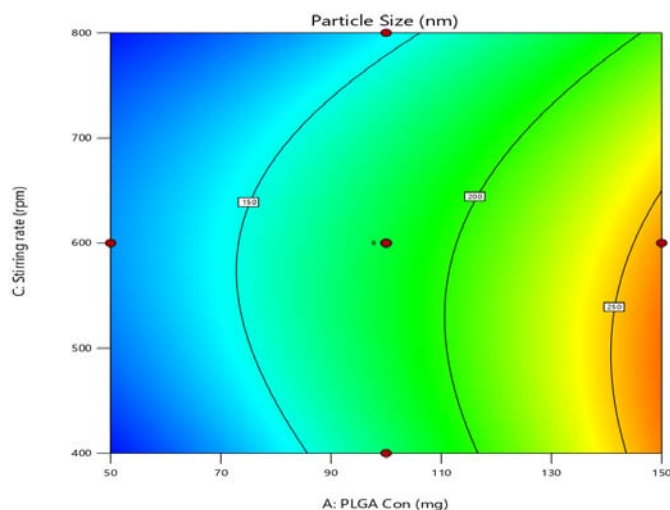


Fig. 1c: 2D Contour plot for particle size as a function of the formulation variables: (A) concentration of PLGA and (C) Stirring rate

Effect of factors on drug entrapment efficiency (R2)

The generated polynomial equation from the quadratic model in terms of coded factors for response R2 drug entrapment efficiency is shown in equation. 4

$$R2 = 85.57 + 11.53A + 3.17B + 1.14C - 0.7363AC - 0.8413BC + 1.19A^2 - 1.68B^2 - 3.10C^2 \text{ equation. 4}$$

As per the coefficients in terms of coded factors from the above equation 3 and their signs, it is evident that individual impact factors A, B, C, A² square coefficient of concentration of PLGA have a significant positive effect and interaction terms AC, BC, and square coefficients B², C² have a negative effect on drug entrapment efficiency. It was found that the effect of PLGA concentration was greater than the change in concentration of PVA and stirring rate on drug entrapment efficiency. The effect of the three variables on the drug entrapment efficiency can be arranged in the sequence A>B>C. Hence, the drug entrapment efficiency will increase with an increase in all three factors [39].

Favipiravir was highly soluble in the organic phase, showing higher polymer interactions with increasing PLGA concentration and

getting maximum entrapment. Moreover, increased PLGA concentration leads to increased particle size, which provides a larger particle volume for favipiravir into nanoparticles, thereby increasing the drug entrapment efficiency. Moreover, as discussed earlier, an increase in polymer concentration increases the organic phase viscosity, which will resist the diffusion of drugs into the aqueous phase, leading to the incorporation of more drugs into nanoparticles [40]. An increase in the concentration of the PVA increased the drug entrapment efficiency due to an increase in the solubility of the drug [41]. The drug entrapment efficiency increases when the stirring rate is increased due to the fact that a unidirectional and less turbulent flow in the case of lower speed may have resulted in the loss of the drug from the organic phase.

To visualise the relationship between drug entrapment efficiency and formulation attributes, model graphs, namely perturbation charts, three-dimensional surface plots, and contour plots, were generated. From perturbation chart fig. 2a, it is evident that drug entrapment efficiency increases with an increase in all three factors. A three-dimensional surface plot fig. 2b and contour plot fig. 2c portrays the effect of individual impact factors A, B, and C on drug entrapment efficiency [37].

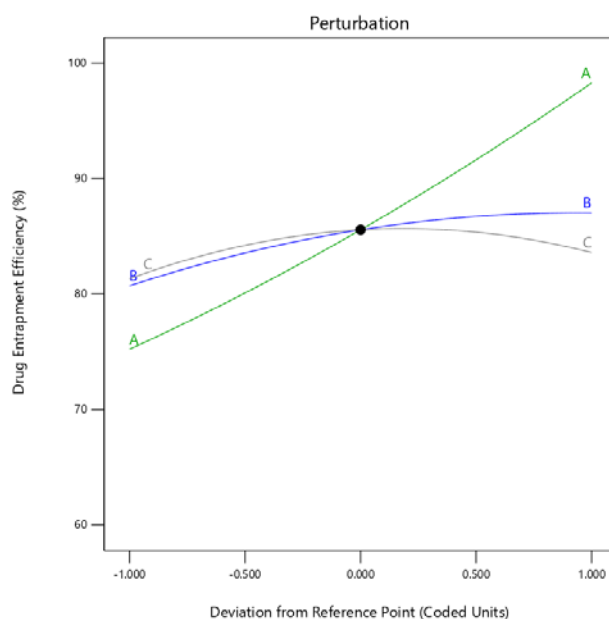


Fig. 2a: Perturbation chart of drug entrapment efficiency

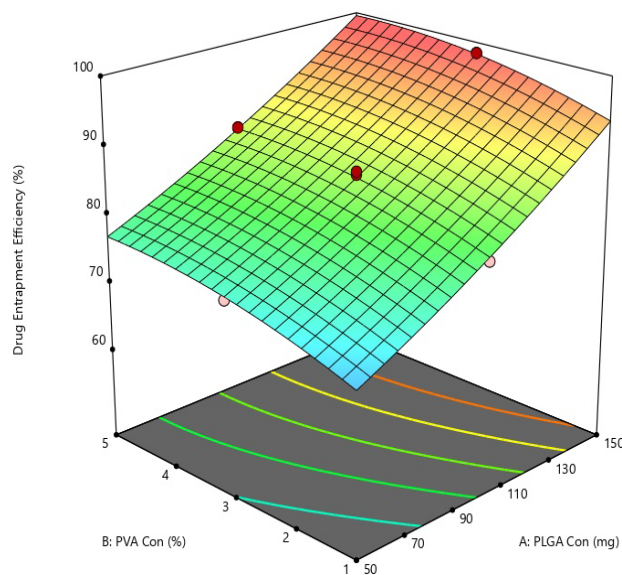


Fig. 2b: Three-dimensional surface plot for drug entrapment efficiency as a function of the formulation variables: (A) concentration of PLGA and (B) concentration of PVA

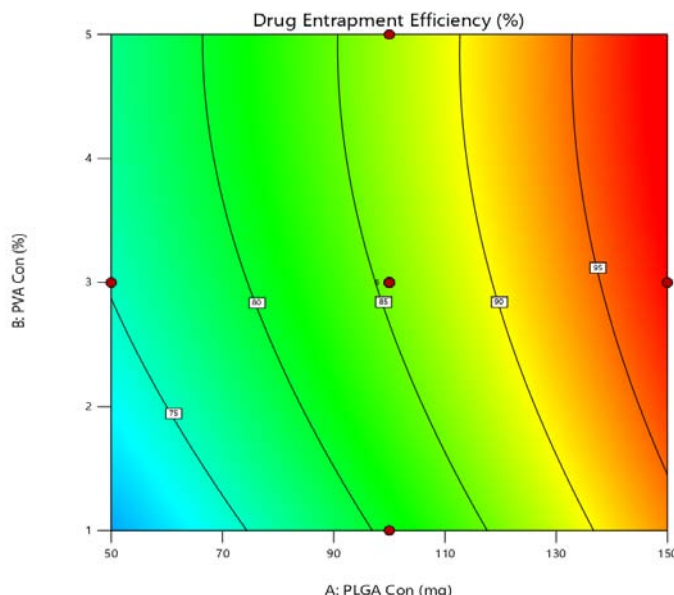


Fig. 2c: 2D Contour plot for drug entrapment efficiency as a function of the formulation variables: (A) concentration of PLGA and (B) concentration of PVA

Effect of factors on cumulative percentage drug release at 720 min (R3)

The polynomial equation from the quadratic model in terms of coded factors for response R3 cumulative percentage drug release at 720 min is shown in Equation. 5.

$$R3 = 79.94 - 13.88A - 1.49B + 1.92AC - 1.97BC - 6.91B^2 + 6.71C^2 \dots\dots \text{Eq. 5.}$$

The coefficient estimated value of the concentration of PLGA (A) was found to be negative, which indicates that the cumulative percentage drug release at 720 min increases with respect to the decrease in the corresponding variable. The antagonist effect was noticed with respect to the concentration of PVA (B) [42].

An increase in PLGA concentration leads to the slow release of favipiravir from the nanoparticles. The reason for the reduction in the cumulative percentage drug release was the formation of thicker

PLGA nanoparticles. Larger particles exhibited a slower rate of drug release due to the longer diffusion pathways that the drug had to travel to reach the dissolution medium [43]. The cumulative percentage drug release decreased with an increase in the PVA concentration [37]. Stirring rate (C) shows no significant effect on cumulative percentage drug release and similar results were reported by Jyosna D *et al.* [44].

To visualise the relationship between cumulative percentage drug release at 720 min and formulation attributes, model graphs, namely perturbation charts, three-dimensional surface plots, and contour plots, were generated. From the perturbation chart fig. 3a, it is evident that an increase in PLGA concentration leads to a decreased cumulative percentage of drug release. A three-dimensional surface plot fig. 3b and contour plot fig. 3c portrays the effect of individual impact factors A, B, and C on the cumulative percentage of drug release at 720 min [44].

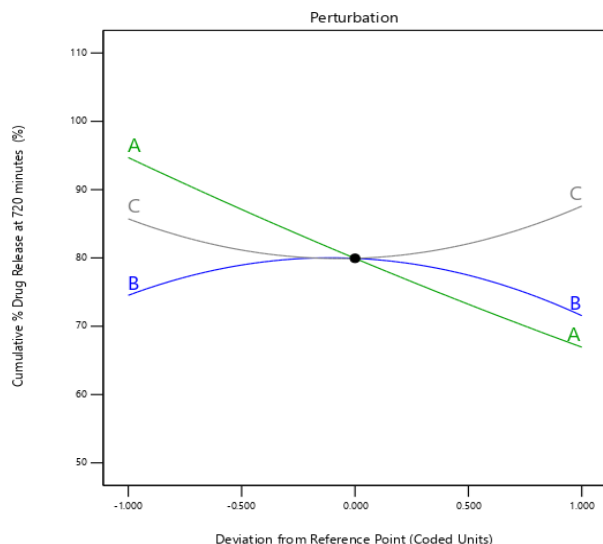


Fig. 3a: Perturbation chart of cumulative percentage drug release at 720 min

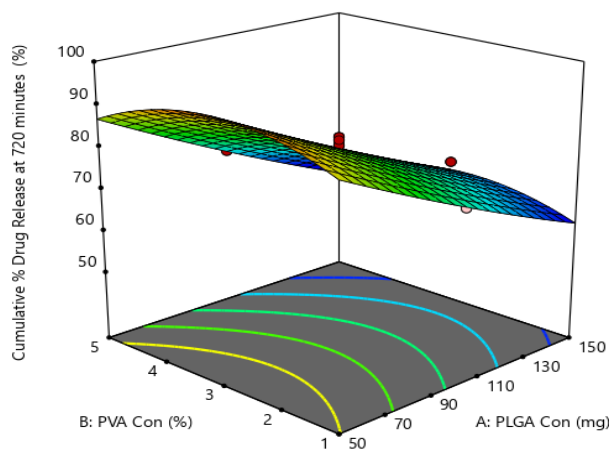


Fig. 3b: Three-dimensional surface plot for cumulative percentage drug release at 720 min as a function of the formulation variables: (A) concentration of PLGA and (B) concentration of PVA

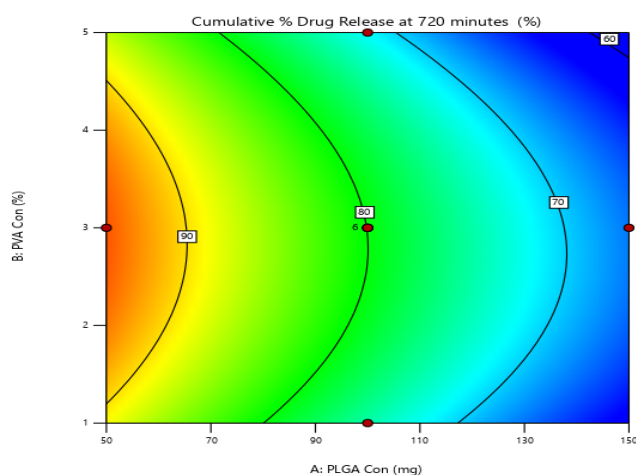


Fig. 3c: 2D Contour plot for cumulative percentage drug release at 720 min as a function of the formulation variables: (A) concentration of PLGA and (B) concentration of PVA

Numerical and graphical optimisation

The optimised favipiravir-loaded PLGA nanoparticles processing conditions with 0.968 desirability were suggested by the Design-

Expert software (Version 13.0.12.0 Trail, Stat Ease Inc, USA). An optimised formulation with optimised conditions was derived with the help of the desirability plot and ramp solutions shown in fig. 4. The optimised formulation was prepared using an optimised PLGA

concentration of 69.96 mg, a PVA concentration of 4.99% and a stirring rate of 799 rpm. This formulation was prepared and its particle size, drug entrapment efficiency, and cumulative percentage drug release at 720 min were determined. The experimental values of responses are compared with the predicted values obtained from

the desirability function, and a relative error was calculated. The results are presented in table 6. The low magnitude of relative error, less than ±2%, confers the robustness and predictability of software in preparing the stable Favipiravir-loaded PLGA nanoparticles [38, 44].

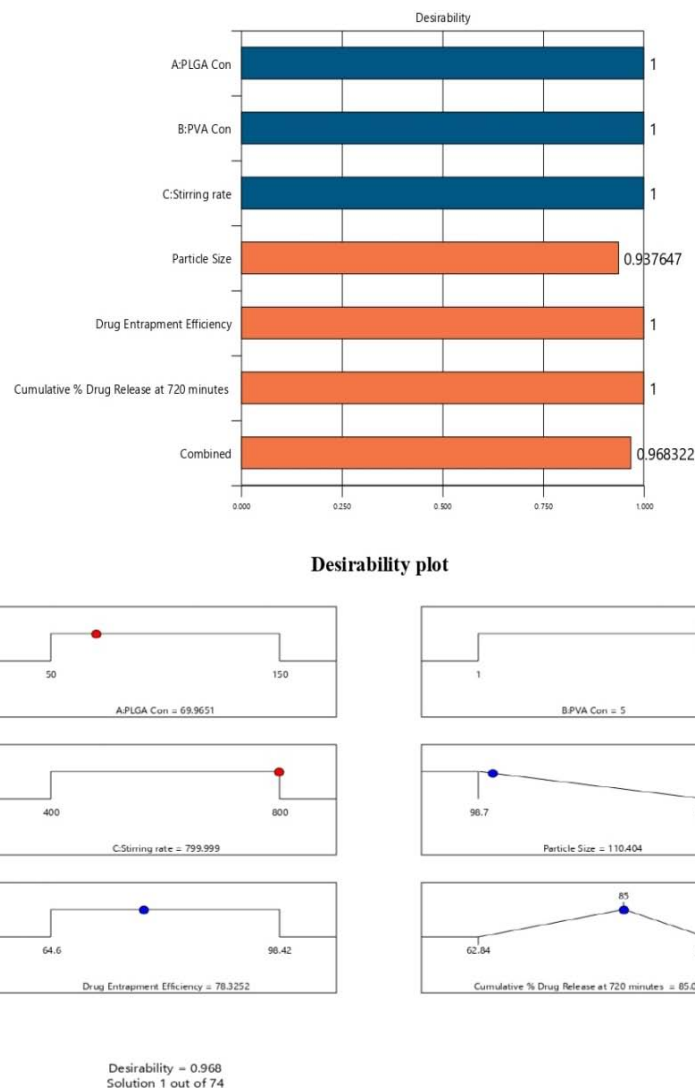


Fig. 4: Desirability plot and ramp solutions for optimization of favipiravir-loaded PLGA nanoparticles

Table 6: Comparison of predicted values and experimental values of responses under optimum conditions

Optimised formulation	A: PLGA concentration (mg)	B: PVA Concentration (%)	C: Stirring rate (rpm)	Responses	Predicted values	Experimental values	Relative error (%)
FNP021	69.96	4.99	799	R1	110.4	109.7	0.634
				R2	78.32	77.65	0.855
				R3	85.00	86.46	-1.717

Characterisation of favipiravir loaded plga nanoparticles

Fourier transform infra-red spectroscopy

FTIR spectra of pure favipiravir and an optimised formulation of favipiravir-loaded PLGA nanoparticles were recorded and represented in fig. 5, fig. 6, respectively. Favipiravir was observed at 3345.95 cm⁻¹ for amine stretching; 1657.83 cm⁻¹ for C=O stretching;

1466.29 cm⁻¹ for C=C stretching; and 1178.02 cm⁻¹ for C-F stretching. The characteristic bands for amine stretching are 3354.27 cm⁻¹, 1687.18 cm⁻¹ for C=O stretching, 1440.79 cm⁻¹ for C=C stretching, and 1186.42 cm⁻¹ for C-F stretching in the optimised formulation. This result indicated that there was no interaction between favipiravir and polymers during the preparation of favipiravir-loaded PLGA nanoparticles [22, 24].

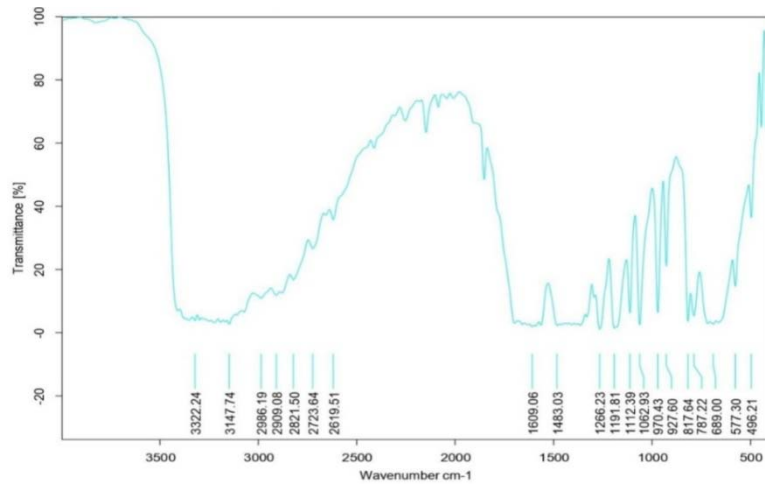


Fig. 5: FTIR spectra of pure favipiravir

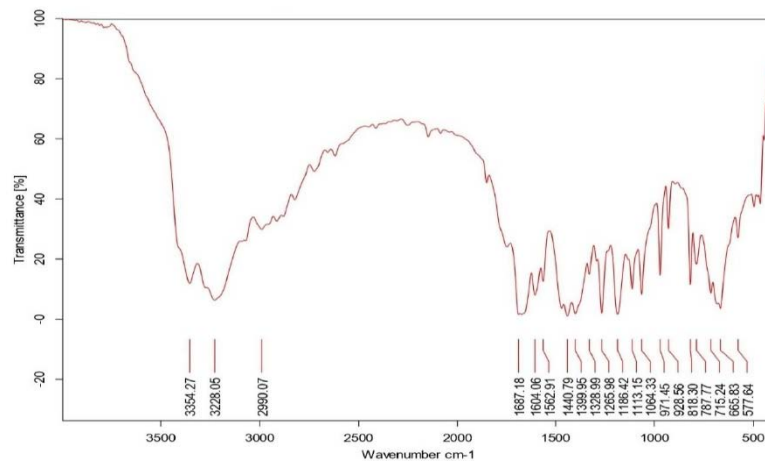


Fig. 6: FTIR spectra of favipiravir-loaded PLGA nanoparticles

Differential scanning calorimetry

DSC thermogram of pure unprocessed favipiravir and the optimised formulation was found to be 199.04 °C and 195.89 °C respectively and is represented in fig. 7, fig. 8. The thermogram of pure favipiravir

exhibits a sharp endothermic peak at 199.04 °C, which corresponds to the melting point of favipiravir. It is considered that the slight change in the endothermic peak of the optimised formulation suggests that favipiravir is only physically entrapped in the polymer matrix but there is no interaction between the drug and the polymer [23, 45].

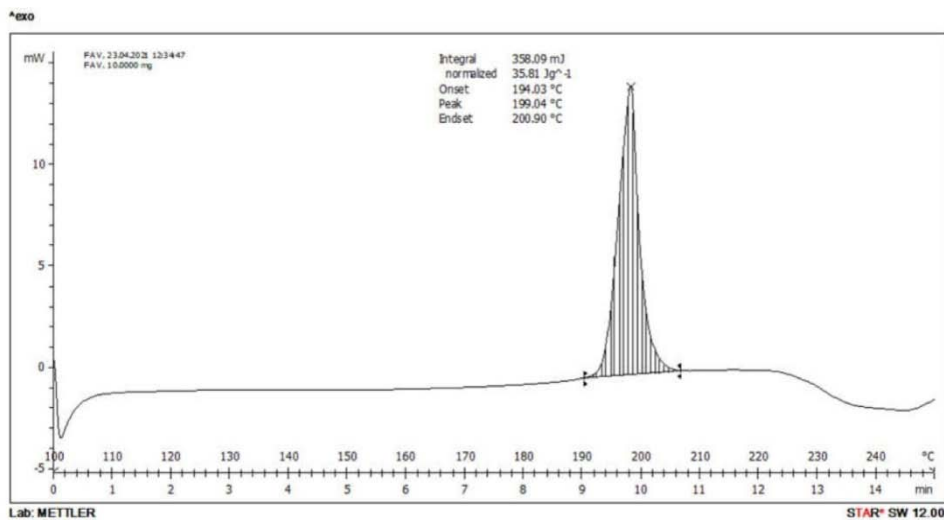


Fig. 7: DSC thermogram of pure favipiravir

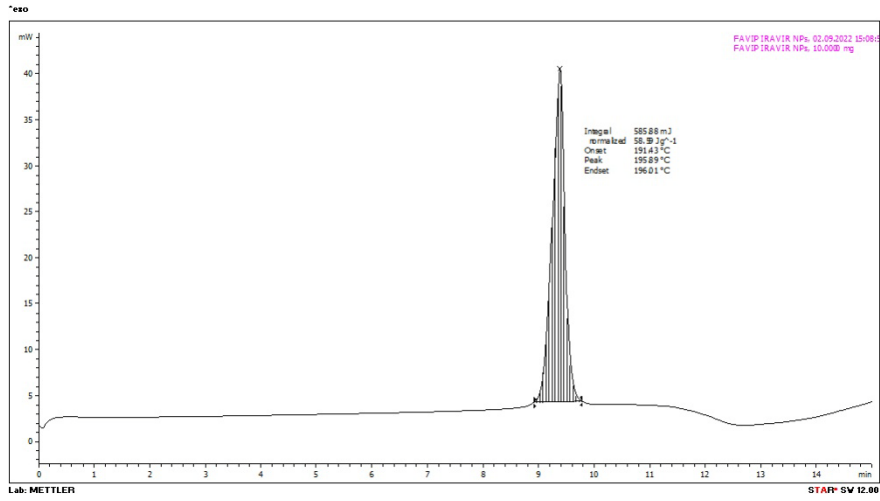


Fig. 8: DSC thermogram of favipiravir loaded PLGA nanoparticles

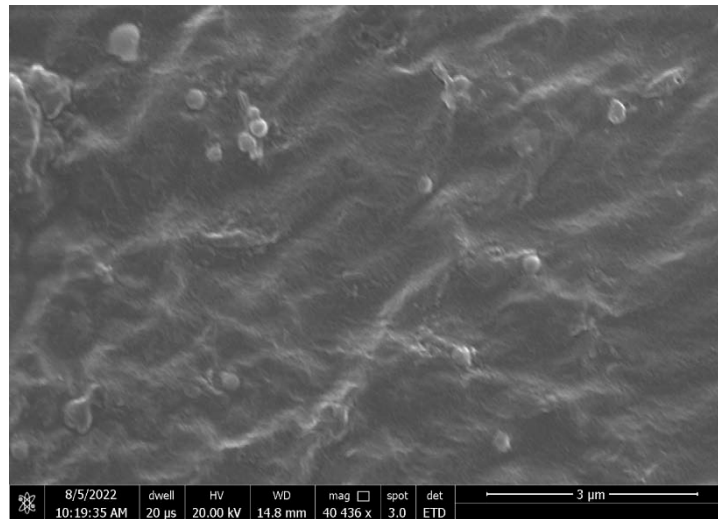


Fig. 9: SEM Image of favipiravir-loaded PLGA nanoparticles

Calculation Results

Peak No.	S.P.Area Ratio	Mean	S. D.	Mode
1	1.00	109.7 nm	41.4 nm	98.9 nm
2	---	--- nm	--- nm	--- nm
3	---	--- nm	--- nm	--- nm
Total	1.00	109.7 nm	41.4 nm	98.9 nm

Cumulant Operations
 Z-Average : 4935.0 nm
 PI : 0.454

Molecular weight measurement
 Molecular weight : ---
 Mark-Houwink-Sakurada parameters : ---

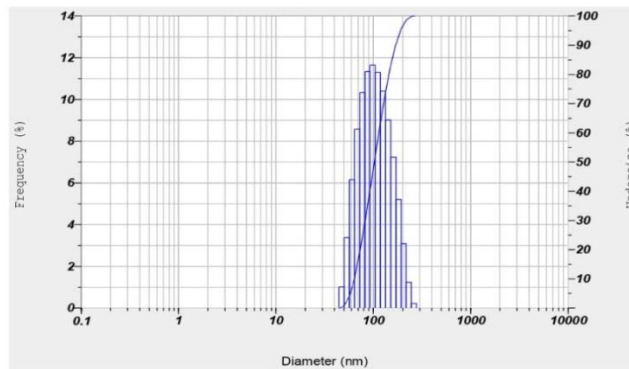
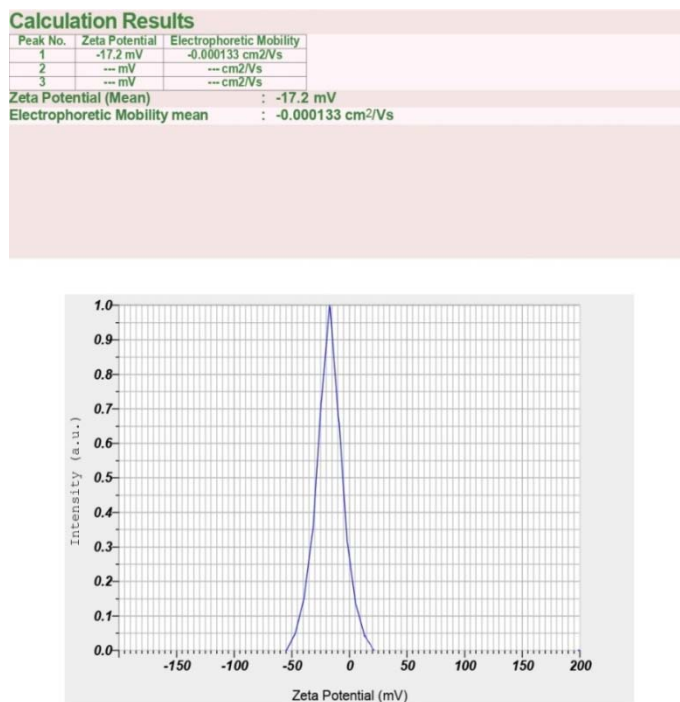


Fig. 10: Particle size of favipiravir-loaded PLGA nanoparticles FNP021



1 / 1

Fig. 11: Zeta potential of favipiravir-loaded PLGA nanoparticles FNP021

Surface morphology

The SEM image of the optimised formulation of favipiravir-loaded PLGA nanoparticles is depicted in fig. 9. The micrographs show that the prepared nanoparticles were nearly spherical in shape [46].

Particle size, polydispersity index and zeta potential

The particle size was determined for all the prepared favipiravir-loaded PLGA nanoparticles. The mean particle sizes of all formulations (FNP01-FNP020) were found to be in the range of 98.7 to 286.4 nm. The mean particle size of optimised formulation FNP021 was found to be in the size range of 109.7 nm as shown in fig. 10 with a polydispersity index of 0.454 and a zeta potential of -17.2 mV as represented in fig. 11. It is reported that nanoparticles

with negative zeta potential are less prone to aggregation and indicates good stability [47].

In vitro drug release testing

A slow release of favipiravir from nanoparticles was observed in 50 mmol phosphate buffer of pH 6.8, which was sustained for up to 720 min. The cumulative percentage drug release of all the formulations was in the range of 62.84 to 97.62 % shown in table 7. The cumulative percentage drug release profiles of FNP01 to FNP010 formulations were shown in fig. 12 and for FNP011 to FNP021 formulations, they were shown in fig. 13. Larger particles exhibited a slower rate of drug release due to the longer diffusion pathways that the drug had to travel to reach the dissolution medium [43].

Table 7: Cumulative percentage drug release of favipiravir-loaded PLGA nanoparticles-experimental formulations [FNP01 to FNP021]

Formulation code	30 min	60 min	120 min	240 min	360 min	480 min	600 min	720 min
FNP01	2.60±0.31	8.48±0.17	16.38±1.05	26.74±0.28	36.86±1.35	44.37±0.08	53.96±0.87	62.84±0.54
FNP02	16.72±0.15	24.36±0.26	38.35±1.28	57.48±0.06	64.32±0.28	73.50±0.69	86.28±0.56	96.45±0.17
FNP03	5.64±0.29	10.38±0.36	19.98±0.43	28.34±0.08	36.89±1.08	44.78±0.96	51.36±0.27	68.89±0.44
FNP04	3.69±0.54	8.46±1.02	15.85±0.28	27.32±0.09	40.36±0.15	48.84±0.04	56.37±0.19	71.65±0.58
FNP05	4.86±0.42	12.58±0.06	20.34±0.72	30.59±0.48	42.48±0.64	49.82±1.05	62.50±0.27	73.56±0.94
FNP06	12.16±0.64	23.28±0.39	36.59±1.12	51.63±0.57	65.46±0.96	74.82±0.89	83.66±0.38	94.58±1.08
FNP07	6.46±0.49	15.83±0.07	26.86±0.25	34.68±0.14	45.92±0.08	58.42±0.35	66.58±0.23	78.39±0.96
FNP08	9.26±0.35	16.34±0.15	30.89±0.22	43.18±0.94	52.68±1.23	63.52±0.07	70.36±0.44	85.49±1.32
FNP09	6.26±0.21	14.93±0.66	23.64±0.59	32.82±0.32	44.29±0.47	52.98±0.34	64.86±0.96	74.25±0.73
FNP010	5.20±0.42	12.46±1.02	22.65±0.18	38.94±0.82	47.68±0.63	54.26±0.75	62.58±0.52	78.25±0.84
FNP011	3.26±0.25	9.84±1.65	19.38±1.48	34.68±0.05	45.92±0.29	58.52±0.57	66.84±0.14	78.39±0.95
FNP012	7.20±0.76	13.86±0.61	23.24±0.05	45.92±2.54	54.84±0.95	61.38±0.58	73.26±0.17	81.89±0.04
FNP013	11.21±0.53	20.36±0.10	33.98±0.78	49.39±0.05	62.73±0.42	75.84±1.25	81.37±0.94	92.56±0.41
FNP014	7.36±0.36	13.58±0.02	22.86±1.14	36.18±0.91	49.73±0.84	58.96±0.67	73.89±0.72	82.61±0.17
FNP015	4.86±0.48	12.86±0.39	20.38±0.11	30.96±0.25	42.48±0.07	49.82±0.18	62.37±0.40	73.56±2.70
FNP016	7.25±0.64	14.48±0.43	22.65±0.16	48.37±0.04	56.48±0.23	64.54±0.11	72.96±0.07	80.62±0.97
FNP017	15.98±1.72	22.30±0.84	36.50±0.32	59.32±0.95	66.72±0.22	77.83±0.48	88.34±0.14	97.62±0.73
FNP018	2.98±0.18	9.68±0.27	18.34±0.52	27.62±0.22	35.38±0.36	43.92±0.18	54.38±1.20	62.98±0.65
FNP019	3.24±0.27	10.35±0.36	19.86±0.82	28.37±0.40	34.98±0.15	42.84±1.24	51.86±0.18	65.68±0.76
FNP020	10.24±0.58	18.86±0.35	39.64±1.48	53.83±0.54	60.96±0.42	72.37±0.67	80.96±0.92	91.47±0.74
FNP021	9.38±0.91	17.86±1.02	32.78±0.65	46.85±0.36	58.10±0.19	69.25±0.48	75.92±0.18	86.46±0.54

(Values represent mean±SD, n=3)

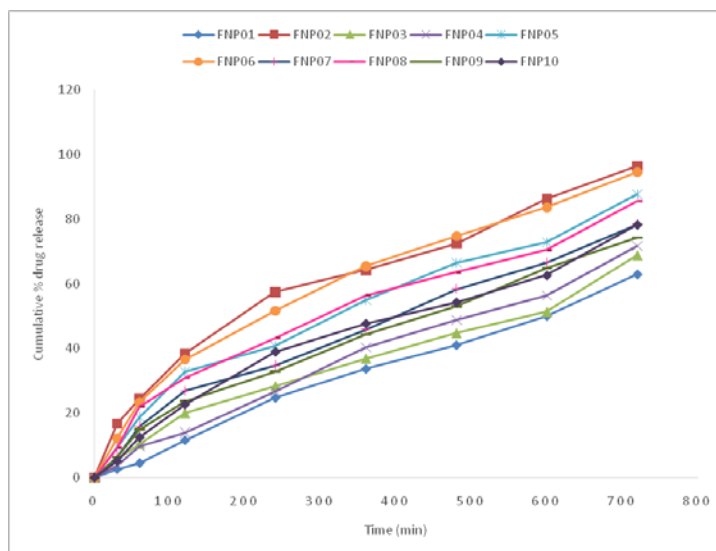


Fig. 12: Cumulative percentage drug release of favipiravir from FNP01 to FNP10 formulations

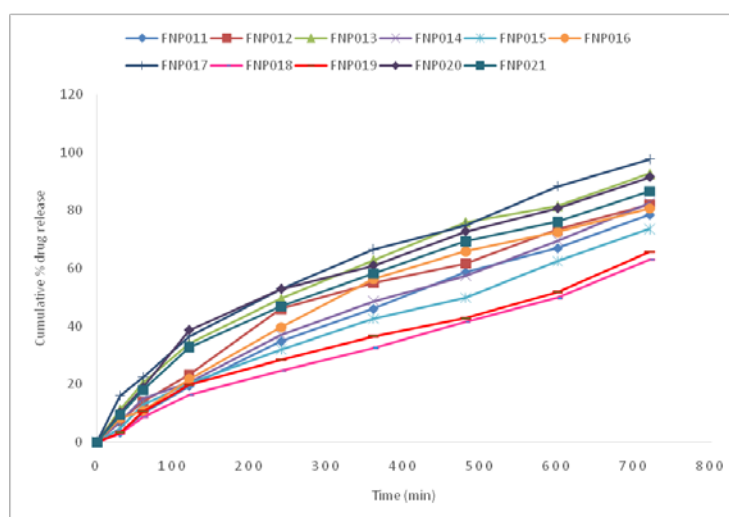


Fig. 13: Cumulative percentage drug release of favipiravir from FNP011 to FNP021 formulations

Kinetic release mechanism

The *in vitro* drug release kinetics of optimised formulation FNP021 was analysed by zero-order, first-order, Higuchi, and Korsmeyer peppas models and their plots are shown in fig. 14–17. The kinetics of drug release of optimised formulation FNP021 were presented in table 8. The optimised formulation of favipiravir-loaded PLGA nanoparticles followed first-order release kinetics with a regression coefficient (R^2) of 0.989 when compared to the zero-order release kinetics with a regression coefficient (R^2) of 0.887. The regression coefficient (R^2) value

was relatively higher in the first-order model, indicating that the drug release followed first-order kinetics. The drug release mechanism of favipiravir-loaded PLGA nanoparticles FNP021 was studied by comparing the Higuchi and Korsmeyer peppas models. Korsmeyer peppas model of optimised formulation FNP021 showed good linearity with a regression coefficient (R^2) of 0.995 and a diffusional exponent "n" value of 0.690, indicating an anomalous non-fickian diffusion mechanism, in which favipiravir is released by diffusion and relaxation of polymer occurs simultaneously. The favipiravir release from nanoparticles follows first-order kinetics with non-fickian diffusion [24].

Table 8: Kinetics of drug release of optimised formulation FNP021 of favipiravir-loaded PLGA nanoparticles

Time (min)	Cumulative % drug release	Cumulative % drug retained	log Cumulative % drug release	log cumulative % drug retained	log time	\sqrt{T}
0	0	0	0	0	0	0
30	9.38	90.62	0.97	1.95	1.47	5.47
60	17.86	82.14	1.25	1.91	1.77	7.74
120	32.78	67.22	1.51	1.83	2.07	10.95
240	46.85	53.15	1.67	1.72	2.38	15.49
360	58.10	41.90	1.76	1.62	2.55	18.97
480	69.25	30.75	1.84	1.48	2.68	21.90
600	75.92	24.08	1.88	1.38	2.77	24.49
720	86.46	13.54	1.93	1.13	2.85	26.83

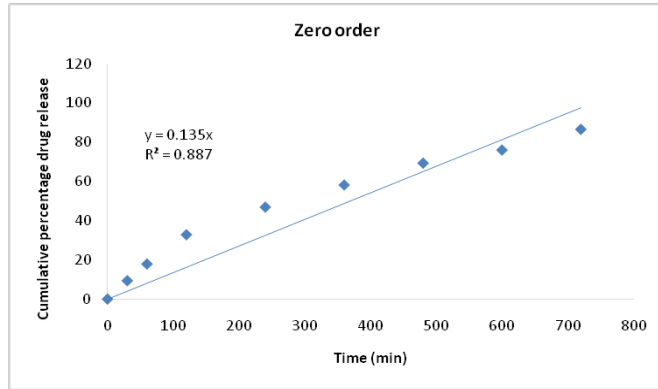


Fig. 14: Zero order plot of optimised favipiravir-loaded PLGA nanoparticle formulation FNP021

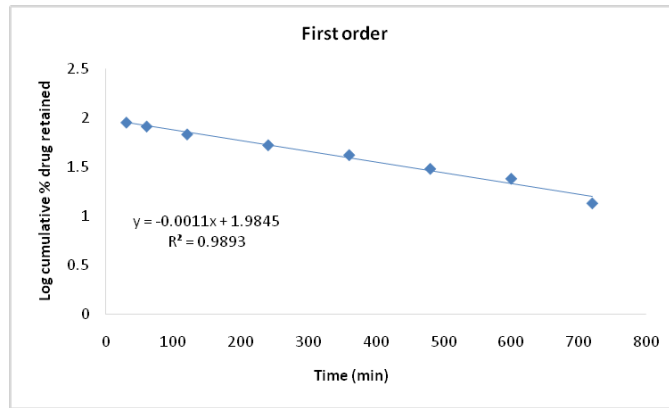


Fig. 15: First order plot of optimised favipiravir-loaded PLGA nanoparticle formulation FNP021

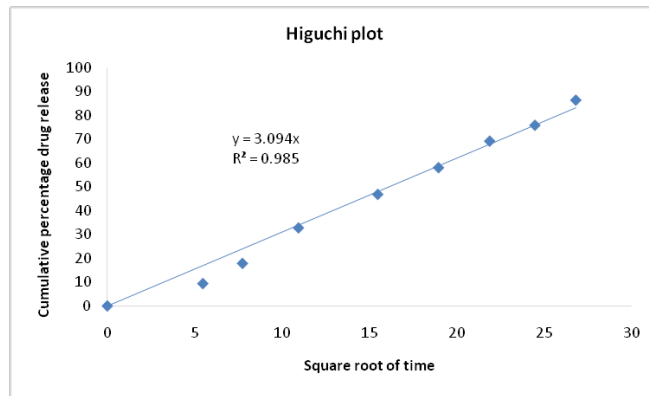


Fig. 16: Higuchi plot of optimised favipiravir-loaded PLGA nanoparticle formulation FNP021

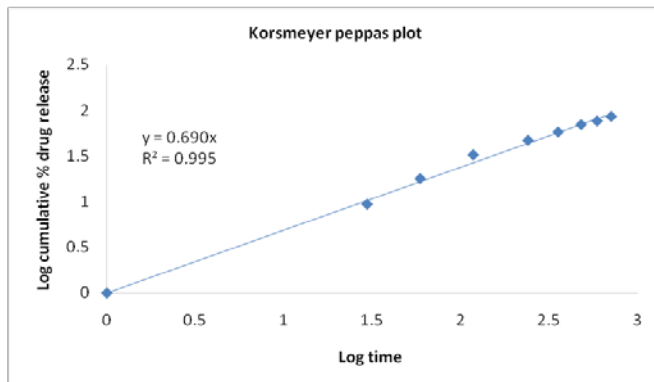


Fig. 17: Korsmeyer peppas plot of optimised favipiravir-loaded PLGA nanoparticle FNP021

CONCLUSION

A satisfactory attempt was made to develop favipiravir polymeric nanoparticles by employing a nanoprecipitation method using PLGA as the polymer and PVA as the stabilizer. A 3 factor, 2 level, the face-centered central composite design was adopted for optimisation using Design-Expert software (Version 13.0.12.0 Trail, Stat Ease Inc, USA). The favipiravir-loaded nanoparticles were smooth and spherical in shape, according to a microscopic image. The particle size of optimised nanoparticles was in nanosized 109.7 nm with -17.2 mV zeta potential, which indicates good stability. An *in vitro* drug release study of the optimised favipiravir-loaded PLGA nanoparticle showed sustained release for a prolonged time period. It follows first-order release kinetics and follows anomalous non-fickian diffusion. It is concluded from the results that the prepared favipiravir-loaded PLGA nanoparticles could be promising formulations for effective favipiravir delivery.

ACKNOWLEDGEMENT

Authors are thankful to Sri Padmavati Mahila University for providing facilities to carry out research work.

FUNDING

This research did not receive a specific grant from any funding agencies.

AUTHORS CONTRIBUTIONS

This work was carried out in collaboration between both authors. Both authors read and approved the final manuscript.

CONFLICT OF INTERESTS

The authors declare no conflict of interest.

REFERENCES

- Joshi S, Parkar J, Ansari A, Vora A, Talwar D, Tiwaskar M. Role of favipiravir in the treatment of COVID-19. *Int J Infect Dis*. 2021;102:501-8. doi: 10.1016/j.ijid.2020.10.069. PMID 33130203.
- Chen R, Wang T, Song J, Pu D, He D, Li J. Antiviral drug delivery system for enhanced bioactivity, better metabolism and pharmacokinetic characteristics. *Int J Nanomedicine*. 2021;16:4959-84. doi: 10.2147/IJN.S315705. PMID 34326637.
- Łagocka R, Dziejewski V, Kłos P, Pawlik A. Favipiravir in therapy of viral infections. *J Clin Med*. 2021;10(2):273-89. doi: 10.3390/jcm10020273, PMID 33451007.
- Pathak S, Vyas SP, Pandey A. Development, characterization and *in vitro* release kinetic studies of ibandronate loaded chitosan nanoparticles for effective management of osteoporosis. *Int J App Pharm*. 2021;13(6):120-5. doi: 10.22159/ijap.2021v13i6.42697.
- Faridi Esfanjani A, Jafari SM. Biopolymer nanoparticles and natural nano-carriers for nano-encapsulation of phenolic compounds. *Colloids Surf B Biointerfaces*. 2016;146:532-43. doi: 10.1016/j.colsurfb.2016.06.053. PMID 27419648.
- Bohrey S, Chourasiya V, Pandey A. Polymeric nanoparticles containing diazepam: preparation, optimization, characterization, *in vitro* drug release and release kinetic study. *Nano Converg*. 2016;3(1):3. doi: 10.1186/s40580-016-0061-2, PMID 28191413.
- Tripathi SK, Patel B, Shukla S, Pachouri C, Pathak S, Pandey A. Donepezil loaded PLGA nanoparticles, from modified nanoprecipitation, an advanced drug delivery system to treat alzheimer disease. *J Phys: Conf Ser*. 2021;1849(1):012001. doi: 10.1088/1742-6596/1849/1/012001.
- Tulbah AS, Hin Lee WH. Physicochemical characteristics and *in vitro* toxicity/anti-SARS-CoV-2 activity of favipiravir solid lipid nanoparticles (SLNs). *Pharmaceuticals (Basel)*. 2021;14(10):1059-72. doi: 10.3390/ph14101059, PMID 34681283.
- Yao Chun, Xiang F, Xu Zhangyi. Metal oxide nanocage as drug delivery systems for favipiravir, as an effective drug for the treatment of COVID-19: a computational study. *J Mol Model*. 2022;28(3):64. doi: 10.1007/s00894-022-05054-6, PMID 35182223.
- Shaik NB, Pk L, Vv BR. Formulation and evaluation of favipiravir proliposomal powder for pulmonary delivery by nebulization. *Int J Pharm Res Allied Sci* 2022;11(2):36-44. doi: 10.51847/4McfhPccXs.
- Avinash D, Gudipati M, Ramana MV, Vadlamudi P, Nadendla RR. Mouth dissolving tablets of favipiravir using superdisintegrants: preparation, optimization and *in vitro* evaluation. *JPRI* 2021;33:28-39. doi: 10.9734/jpri/2021/v33i631187.
- Danhier F, Ansorena E, Silva JM, Coco R, Le Breton A, Preat V. PLGA-based nanoparticles: an overview of biomedical applications. *J Control Release*. 2012;161(2):505-22. doi: 10.1016/j.jconrel.2012.01.043. PMID 22353619.
- Venkatesh DN, Baskaran M, Karri VV, Mannemala SS, Radhakrishna K, Goti S. Fabrication and *in vivo* evaluation of nelfinavir loaded PLGA nanoparticles for enhancing oral bioavailability and therapeutic effect. *Saudi Pharm J*. 2015;23(6):667-74. doi: 10.1016/j.jsps.2015.02.021. PMID 26702262.
- Yadav KS, Sawant KK. Modified nanoprecipitation method for preparation of cytarabine-loaded PLGA Nanoparticles. *AAPS PharmSciTech*. 2010;11(3):1456-65. doi: 10.1208/s12249-010-9519-4, PMID 20842542.
- Todaro B, Moscardini A, Luin S. Pioglitazone-loaded PLGA nanoparticles: towards the most reliable synthesis method. *Int J Mol Sci*. 2022;23(5):2522-6. doi: 10.3390/ijms23052522, PMID 35269665.
- Sebastian G, Priya S, P James, MA Sannidhi, Prabhu VK, Sannidhi, Vinay Kiran Prabhu. Computational tools assisted formulation optimization of nebigolol hydrochloride loaded PLGA nanoparticles by 3²factorial designs. *Int J App Pharm*. 2022;14(4):251-8. doi: 10.22159/ijap.2022v14i4.44865.
- Saka OM, Oz UC, Kucukturkmen B, Devrim B, Bozkır A. Central composite design for optimization of zoledronic acid loaded PLGA nanoparticles. *J Pharm Innov*. 2020;15(1):3-14. doi: 10.1007/s12247-018-9365-6.
- Varshosaz J, Ghaffari S, Khoshayand MR, Atyabi F, Azarmi S, Kobarfard F. Development and optimization of solid lipid nanoparticles of amikacin by central composite design. *J Liposome Res*. 2010;20(2):97-104. doi: 10.3109/08982100903103904, PMID 19621981.
- Panda BP. Impact of Statistical Central Composite Face Centered Design Approach on Method and Process Optimization of Metformin Hydrochloride Loaded PLGA Nanoformulation. *Micro Nanosystems*. 2017;9(1):55-71. doi: 10.2174/1876402909666170817113542.
- mali S, oza N. Central composite design for formulation and optimization of long-acting injectable (LAI) microspheres of paliperidone palmitate. *Int J App Pharm*. 2021;13(5):87-98. doi: 10.22159/ijap.2021v13i5.42297.
- Hassan H, Adam SitiK, Alias E, Meor Mohd Affandi MMR, Shamsuddin AF, Basir R. Central composite design for formulation and optimization of solid lipid nanoparticles to enhance oral bioavailability of acyclovir. *Molecules*. 2021;26(18):5432. doi: 10.3390/molecules26185432, PMID 34576904.
- Yadav M, Aggarwal P, Yadav D, Singh A. Formulation and evaluation of clobetasol-17-propionate-loaded carboxymethyl chitosan nanoparticle. *Asian J Pharm Clin Res*. 2022;2022:88-93. doi: 10.22159/ajpcr.2022.v15i9.45743.
- Tiğlı Aydın RS, Kaynak G, Gumusderelioglu M. Salinomycin encapsulated nanoparticles as a targeting vehicle for glioblastoma cells. *J Biomed Mater Res A*. 2016;104(2):455-64. doi: 10.1002/jbm.a.35591. PMID 26476239.
- Naveentaj S, Muzib YI, Radha R. Design and development of simvastatin-loaded pharmacosomes to enhance transdermal permeation. *Int J App Pharm*. 2022;14(4):148-57. doi: 10.22159/ijap.2022v14i4.44527.
- Salmanpour M, Saeed Vaghefi M, Abolmaali SS, Tamaddon AM. Sterically stabilized polyionic complex nanogels of chitosan lysate and PEG-b-Polyglutamic acid copolymer for the delivery of active irinotecan metabolite (SN-38). *Curr Drug Deliv*. 2021;18(6):741-52. doi: 10.2174/1567201817999201103195846, PMID 33155910.

26. Yang H, Li J, Patel SK, Palmer KE, Devlin B, Rohan LC. Design of poly(lactic-co-glycolic acid) (PLGA) nanoparticles for vaginal co-delivery of griffithsin and dapivirine and their synergistic effect for HIV prophylaxis. *Pharmaceutics*. 2019;11(4):184. doi: 10.3390/pharmaceutics11040184, PMID 30995761.
27. Avinash D, Gudipati M, Ramana MV, Vadlamudi P, Nadendla RR. Mouth dissolving tablets of favipiravir using superdisintegrants: preparation, optimization and *in vitro* evaluation. *JPRI* 2021;33:28-39. doi: 10.9734/jpri/2021/v33i631187.
28. Sharma D, Maheshwari D, Philip G, Rana R, Bhatia S, Singh M. Formulation and optimization of polymeric nanoparticles for intranasal delivery of lorazepam using box-behnken design: *in vitro* and *in vivo* evaluation. *BioMed Res Int*. 2014;2014:156010. doi: 10.1155/2014/156010. PMID 25126544.
29. Imtiaz N, Majee SB, Biswas GR. Development and characterization of oral swellable rapid-release film with superdisintegrant-surfactant. *Int J Curr Pharm Sci*. 2021;13(1):75-80. doi: 10.22159/ijcpr.2021v13i1.40821.
30. Zhou YZ, Alany RG, Chuang V, Wen J. Optimization of PLGA nanoparticles formulation containing L-dopa by applying the central composite design. *Drug Dev Ind Pharm*. 2013;39(2):321-30. doi: 10.3109/03639045.2012.681054, PMID 22607101.
31. Wan Maznah Wan Ishak, Mohd Hanif Zulfakar. Optimization, development, and safety evaluation of olive oil nanoemulsion for topical application: a response surface methodology. *Asian J Pharm Clin*. 2022;15(9):167-73. doi: 10.22159/ajpcr.2022.v15i9.45964.
32. Nandy BC, Mazumder B. Formulation and characterizations of delayed-release multi particulates system of indomethacin: optimization by response surface methodology. *Curr Drug Deliv*. 2014;11(1):72-86. doi: 10.2174/15672018113109990041, PMID 24783236.
33. Teja SPS, Damodharan N. 3Full factorial model for particle size optimisation of methotrexate loaded chitosan nanocarriers: A design of experiments (DOE) approach. *BioMed Res Int*. 2018;2018:7834159. doi: 10.1155/2018/7834159, PMID 30356374.
34. Abbas Z, Marihal S. Gellan gum-based mucoadhesive microspheres of almotriptan for nasal administration: formulation optimization using factorial design, characterization, and *in vitro* evaluation. *J Pharm Bioallied Sci*. 2014;6(4):267-77. doi: 10.4103/0975-7406.142959. PMID 25400410.
35. Sahin A, Esendagli G, Yerlikaya F, Caban Toktas S, Yoyen Ermis D, Horzum U. A small variation in average particle size of PLGA nanoparticles prepared by nanoprecipitation leads to considerable change in nanoparticles' characteristics and efficacy of intracellular delivery. *Artif Cells Nanomed Biotechnol*. 2017;45(8):1657-64. doi: 10.1080/21691401.2016.1276924, PMID 28084837.
36. Mainardes RM, Evangelista RC. PLGA nanoparticles containing praziquantel: effect of formulation variables on size distribution. *Int J Pharm*. 2005;290(1-2):137-44. doi: 10.1016/j.ijpharm.2004.11.027. PMID 15664139.
37. Sharma N, Madan P, Lin S. Effect of process and formulation variables on the preparation of parenteral paclitaxel-loaded biodegradable polymeric nanoparticles: a co-surfactant study. *Asian J Pharm Sci*. 2016;11(3):404-16. doi: 10.1016/j.ajps.2015.09.004.
38. Kalidas S, Geetha P. Development and optimization of astragalin-loaded polymeric nanoparticles using central composite factorial design. *Int J App Pharm*. 2022;14(5):69-77. doi: 10.22159/ijap.2022v14i5.44315.
39. Rahbarian M, Mortazavian E, Dorkoosh FA, Rafiee Tehrani M. Preparation, evaluation and optimization of nanoparticles composed of thiolated triethyl chitosan: A potential approach for buccal delivery of insulin. *J Drug Deliv Sci Technol*. 2018;44:254-63. doi: 10.1016/j.jddst.2017.12.016.jddst.2017.12.016.
40. Danaei M, Dehghankhold M, Ataei S, Hasanzadeh Davarani F, Javanmard R, Dokhani A. Impact of particle size and polydispersity index on the clinical applications of lipidic nanocarrier systems. *Pharmaceutics*. 2018;10(2):57. doi: 10.3390/pharmaceutics10020057, PMID 29783687.
41. Ekambaram P, Abdul HS A. Formulation and evaluation of solid lipid nanoparticles of ramipril. *J Young Pharm*. 2011;3(3):216-20. doi: 10.4103/0975-1483.83765, PMID 21897661.
42. Pandey P, Chellappan DK, Tambuwala MM, Bakshi HA, Dua K, Dureja H. Central composite designed formulation, characterization and *in vitro* cytotoxic effect of erlotinib loaded chitosan nanoparticulate system. *Int J Biol Macromol*. 2019;141:596-610. doi: 10.1016/j.ijbiomac.2019.09.023. PMID 31494160.
43. Devi KV, Bhosale UV. Formulation and optimization of polymeric nano drug delivery system of acyclovir using 3² full factorial design. *Int J PharmTech Res*. 2009;1(3):644-53.
44. Doniparthi J, B JJ. Novel tamarind seed gum-alginate-based multi-particulates for sustained release of dalfampridine using response surface methodology. *Int J Biol Macromol*. 2020;144:725-41. doi: 10.1016/j.ijbiomac.2019.11.203. PMID 31843610.
45. Padmasri B, Nagaraju R. Formulation and evaluation of novel insitu gel system in the management of rheumatoid arthritis. *Int J App Pharm*. 2022;14(5):62-8. doi: 10.22159/ijap.2022v14i5.43792.
46. Salmanpour Mohsen, Saeed Vaghefi M, Abolmaali SS, Tamaddon AM. Sterically stabilized polyionic complex nanogels of chitosan lysate and PEG-b-Polyglutamic acid copolymer for the delivery of active irinotecan metabolite (SN-38). *Curr Drug Deliv*. 2021;18(6):741-52. doi: 10.2174/1567201817999201103195846, PMID 33155910.
47. Niharika Girish M, KK. Solid lipid nanoparticles of rebamipide: formulation, characterization and *in vivo* pharmacokinetic evaluation. *Int J App Pharm*. 2022;14(2):143-50. doi: 10.22159/ijap.2022v14i2.42945.